

Characteristics of landslides in western Colorado, USA

Abstract Mass movement can be activated by earthquakes, rapid snowmelt, or intense rainstorms in conjunction with gravity. Whereas mass movement plays a major role in the evolution of a hillslope by modifying slope morphology and transporting material from the slope to the valley, it is also a potential natural hazard. Determining the relationships of frequency and magnitude of landslides are fundamental to understanding the role of landslides in the study of landscape evolution, hazard assessment, and determination of the rate of hillslope denudation. We mapped 735 shallow and active landslides in the Paonia to McClure Pass area of western Colorado from aerial photographs and field surveys. The study area covers $\sim 815\text{km}^2$. The frequency–magnitude relationships of the landslides illustrate the flux of debris by mass movement in the area. The comparison of the probability density of the landslides with the double Pareto curve, defined by power scaling for negative slope (α), power scaling for positive slope (β), and location of rollover (t), shows that $\alpha=1.1$, $\beta=1.9$, and $t=1,600\text{m}^2$ for areas of landslides and $\alpha=1.15$, $\beta=1.8$, and $t=1,900\text{m}^3$ for volumes of landslides. The total area of landslides is $4.8 \times 10^6\text{m}^2$ and the total volume of the landslides is $1.4 \times 10^7\text{m}^3$. The areas (A) and the volumes (V) of landslides are related by $V=0.0254 \times A^{1.45}$. The frequency–magnitude analysis shows that landslides with areas ranging in size from 1,600 to $20,000\text{m}^2$ are the most hazardous landslides in the study area. These landslides are the most frequent and also do a significant amount of geomorphic work. We also developed a conceptual model of hillslope development to upland plateau driven by river incision, shallow landsliding, and deep-seated large landsliding. The gentle slope to flat upland plateau that dominated the Quaternary landscape of the study area was modified to the present steep and rugged topography by the combined action of fluvial incision and glacial processes in response to rock uplift, very-frequent shallow landsliding, and less-frequent deep-seated landsliding.

Keywords Landslides · Frequency-magnitude relationship · Hillslope denudation · Landscape evolution

Introduction

Landslides, complex natural phenomena, are the results of the variety of geomorphic, geologic, and hydrologic factors which predispose hillslopes to instability. Events like earthquakes, intense rainfalls, and snowmelt trigger cascading of mass from slopes (Delgado et al. 2011; Jones and Preston 2012). Landslides play a significant role in the modification of the hillslope by transporting sediments from a slope to the base of that slope (Levy et al. 2012). Most shallow landslides result from triggering by rainfall and earthquakes and are important tools in contributing to sediment yield (Burton and Bathurst 1998; Glade 2003; Lin et al. 2012). The amount of debris mobilized by landslides depends on a combination of the spatial distribution and frequency of triggering events, the number of failures triggered in a given event, the probability distribution of landslide volume for such a triggering event and the flux of the debris from landslides into the channel network (Stark and Guzzetti 2009).

For at least four decades, researchers have been investigating the relationships of magnitudes and frequencies of landslides in different lithological and geomorphological terrains to understand the role of landslides in sediment yield, landscape evolution, and as hazards (Fujii 1969; Whitehouse and Griffiths 1983; Noever 1993; Somfai et al. 1994; Hovius et al. 1997; Pelletier 1997; Crozier 1999; Crozier and Glade 1999; Hovius et al. 2000; Dai and Lee 2001; Stark and Hovius 2001; Guzzetti et al. 2002; Martin et al. 2002; Brardinoni and Church 2004; Guthrie and Evans 2004a, b; Malamud et al. 2004; Korup 2005; Guthrie and Evans 2007; Guzzetti et al. 2008; Stark and Guzzetti 2009; Larsen et al. 2010). The magnitude of a landslide, defined as the capability to produce change and or the energy associated with the detached mass (Corominas et al. 2003), is represented by the area of a landslide scar (Hovius et al. 1997, 2000), the total area of a landslide (Pelletier 1997; Guzzetti et al. 2002), or the volume of the material displaced by a landslide (Hungri et al. 1999; Dai and Lee 2001). Frequency of landslides is defined as the number of landslides related to a single event or the various events that occurred in the past. Almost all investigators obtained a power relationship between the frequencies and magnitudes of landslides. Interestingly, a rollover effect appears on a graph of frequencies and magnitudes. A rollover is a point from where the frequency–magnitude relationships of smaller landslides cannot be explained by the power law representing the frequency–magnitude relation of large- and medium-sized landslides. Reasons for the rollover have generally been attributed to an inability to consistently resolve and map all small landslides at a given scale (Hungri et al. 1999; Stark and Hovius 2001; Brardinoni et al. 2003; Brardinoni and Church 2004), physical condition of the hillslope on which the landslides occur (Pelletier 1997; Hovius et al. 2000; Guzzetti et al. 2002; Martin et al. 2002; Brardinoni and Church 2004; Guthrie and Evans 2004a, b), consequence of material strength limiting the number of small slides and the overall slope geometry that limits the number of very large slides (Pelletier 1997; Guzzetti et al. 2002), and self-organized criticality (Noever 1993; Hergarten and Neugebauer 1998). Pelletier (1997) suggested that the rollover might represent the transition from a resistance controlled by friction (large landslides) to a resistance controlled by cohesion (small landslides).

The geomorphological expression of the landscape develops by the transfer of mass from unstable zones on steep slopes and highlands to fluvial and coastal lowlands by integrated erosional processes of wind, water or ice, and mass movements. Comparatively, landslides transfer considerable volumes of slope material and play an important role in shaping the landscape. In many humid upland landscapes, evolution of the hillslope is dominated by landsliding across a wide range of length scales (Anderson 1994; Gerrard 1994; Greenbaum et al. 1995; Schmidt and Montgomery 1995; Burbank et al. 1996). This nature of landslides can be quantified in terms of the geomorphic work. The work performed by a landslide is defined in terms of destructiveness (Evans 2003; Malamud et al. 2004), fragmentation energy (Locat et al. 2006), runout (Hungri and Evans 2004; McClung 2000), volume (Innes 1983; Hovius et al. 2000; Martin et al. 2002), combination of volume and expected velocity (Cardinali et al.

2002; Reichenbach et al. 2005), or the product of magnitude (size) and frequency or probability of landslide occurrence (Guthrie and Evans 2007). Large landslides displace large volumes of materials and leave geomorphic signatures for many years (Korup 2006; Guthrie and Evans 2007). But the frequency of occurrence of large landslides is very low. In contrast, small landslides are frequent but displace only very small amounts of slope material at a time. Furthermore, the signatures of the small landslides disappear in a short period of time (Guthrie and Evans 2007). Although much research has been done to document the morphology and mechanics, susceptibility and slope stability of landslides, research into the role of magnitudes and frequencies of landslides on the evolution of the landscape is still needed. Recently, a few studies have been conducted on a regional scale to understand the contribution of landslides to landscape evolution (Korup 2006; Guthrie and Evans 2007).

The primary goals of this study are: (a) to determine the characteristics of the shallow landslides in Paonia–McClure Pass area of western Colorado by using frequency–magnitude relationships, (b) assess the area–volume relationships, and (c) assess the geomorphic work of these landslides. To achieve these goals, the following objectives must be met: (1) prepare a landslide inventory map; (2) develop a model that approximates the hillslopes before the landslides occurred and calculate the volume of soil displaced by the landslides; (3) obtain frequency–magnitude relationship curves and compare the frequency–magnitude relationship curves with a double Pareto model to determine the power scaling parameters for small-, medium-, and large-sized shallow landslides; and 4) determine the most important range of the sizes of shallow landslides which yielded most of the sediments. Moreover, the study also estimates the rate of hillslope denudation based on the shallow landslides occurring for the last ~100 years and discusses the geomorphic evolution of the area in terms of the channel incision, shallow landsliding as a process response of channel incision, and the upslope steepening of the hillslopes by deep-seated large landslides.

The study area

The study area, located in west-central Colorado (Fig. 1), extends from Paonia to McClure Pass (N 38°43'00", W 107°37'30" to N 39°10'30", W 107°10'00") and encompasses ~815 km². General access to Paonia–McClure Pass is gained by Colorado Highway 133. Foot trails and forest roads provide access from the highway.

The climate of the study area has average annual temperatures ranging from 1.8 (minimum) to 18 °C (maximum) based on the 1905–2005 data of Paonia 1SW climatic station (Western Regional Climate Center 2012). Precipitation is primarily the result of summer convective thunderstorms. The area also receives winter precipitation in the form of snow. Average annual precipitation is 400 mm based on the 1905–2005 data of Paonia 1SW climatic station (Western Regional Climate Center 2012). Vegetation of the area consists of grasses, aspen groves (*Populus tremuloides*), and pines (*Pinus edulis*). The landcover/landuse in the area is forest, woodland, shrub, and grassland.

Very few studies on landslides have been conducted in the study area. Reconnaissance research on mapping landslides and landslide hazards from Paonia to the Hotchkiss area was completed by Junge (1978) and cover part of the study area. The Colorado Geological Survey studied major landslides and listed the area as

sixth on the 2002 priority list for the Colorado landslide hazard mitigation plan (Rogers 2003). A study on mapping susceptibility to shallow landslides in the area between Paonia and McClure Pass has been performed by Regmi et al. (2010a, b, 2013). But, no study has focused on the frequency–magnitude characteristics of the landslides and the contribution to sediment yield and landscape evolution.

Geomorphology and geology

The area has rugged topography and a dendritic drainage pattern (Fig. 2). The North Fork of the Gunnison River is the major river and drains about 2,500 km² of forested mountainous terrain into the Gunnison River (Jaquette et al. 2005). The elevation ranges from 1,712 to 3,883 m with the lowest elevation on the flood plain of the North Fork of the Gunnison River at Paonia and the highest elevation at Chair Mountain (Fig. 2). The hillslope morphology in the area varies. Most of the small mountains have steep slopes and flat mesa-like tops, whereas mountain highlands have sharp ridges and steep slopes in the form of horns, arêtes, and glacial cirques.

The study area exhibits three different lithologies: (1) Cretaceous sedimentary rocks including sandstone, shale, mudstone, and claystone; (2) Tertiary igneous rocks, including basalt and granodiorites; and (3) various Quaternary deposits all with different geological ages (Fig. 3). Basalt caps many mountains, whereas rocks adjacent to the basalt cap have been stripped away by glaciation, mass movements, and river erosion. These processes left till and colluvium on most of the lowlands and middle slopes. Bedrock is dominant along the steep ridges and fluvial deposits fill the valleys. All processes over long geological time formed the river valleys.

Landslides

The area exhibits two major groups of landslides: (1) shallow landslides and (2) large deep-seated landslides. Shallow landslides are defined as modern (<100 years) and have an area of <160,000 m² and average depth to the slip surface of <10 m. Large deep-seated landslides are defined as paleolandslides (probably hundreds to thousands of years) and have an area of >160,000 m² and average depth to the slip surface of >10 m. Only shallow landslides (Fig. 3) were used to study the frequency–magnitude relationship, area–volume relationship, sediment yield, and geomorphic work of landslides. The large deep-seated landslides (Figs. 2 and 4) were excluded because huge uncertainties will be incorporated into the analysis if landslides of ages ranging from a year to thousands of years were analyzed together. In this study, large deep-seated landslides were used only to discuss the contribution of landslides to landscape evolution.

Shallow landslides (modern landslides)

We mapped 735 distinguishable boundaries (Fig. 3) of shallow landslides (<160,000 m²) including debris flows, debris slides, soil slides, and rockslides from the National Agriculture Imagery Program (NAIP) orthorectified color aerial photographs of 1:12,000 scale acquired in 2005 and US Geological Survey (USGS) black and white orthorectified aerial photographs of 1:12,000 scale acquired in 1993 (Figs. 4 and 6). These landslides, mostly found on 15° to 40° slopes (Fig. 5a), comprised sandstone, mudstone, and colluvial deposits in close proximity to rivers. The area of these landslides ranges from 85 to 1.6 × 10⁵ m², and the average thickness is ~1.9 m (Fig. 5b). Among these landslides, small- and medium-sized landslides occur in

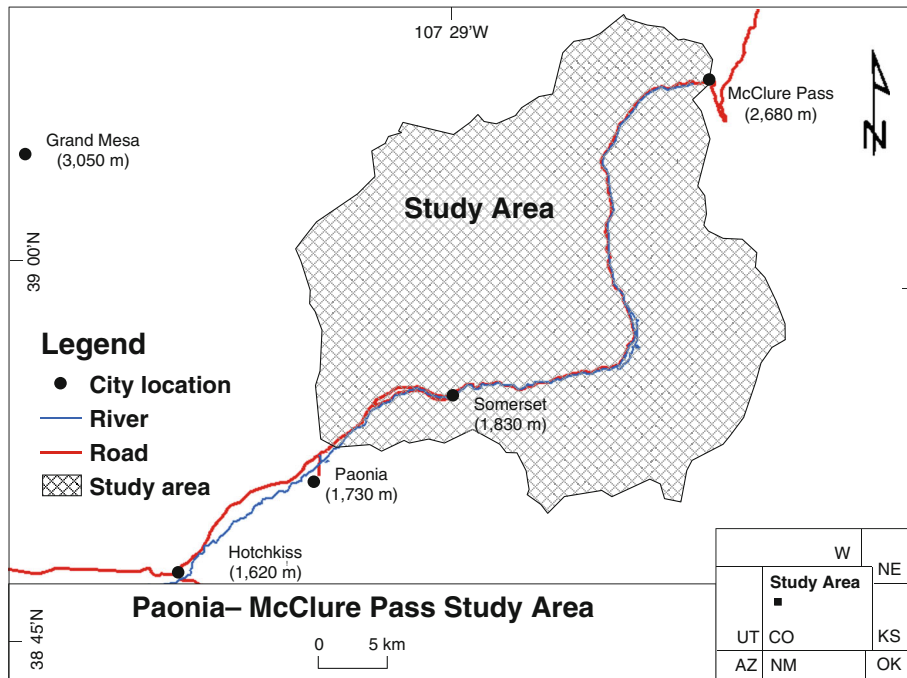


Fig. 1 Paonia–McClure Pass study area. W Wyoming, NE Nebraska, UT Utah, CO Colorado, KS Kansas, AZ Arizona, NM New Mexico, OK Oklahoma

divergent and convergent parts of the slopes, whereas large landslides occur in almost planar parts of the slopes (Fig. 5c). Debris flows mostly occur on the convergent parts of the slopes, rock slides and debris slides occur mostly on planar slopes, and soil slides occur everywhere. Interestingly, most of the larger landslides are rock slides

and most of the smaller landslides are soil slides. Similarly, on average, debris flows have the largest runout length to width ratio and the soil slides have the smallest runout length to width ratio (Fig. 5d).

In areas where soil slides, debris slides, and debris flows occurred, the thin cover of the regolith above the bedrock moved

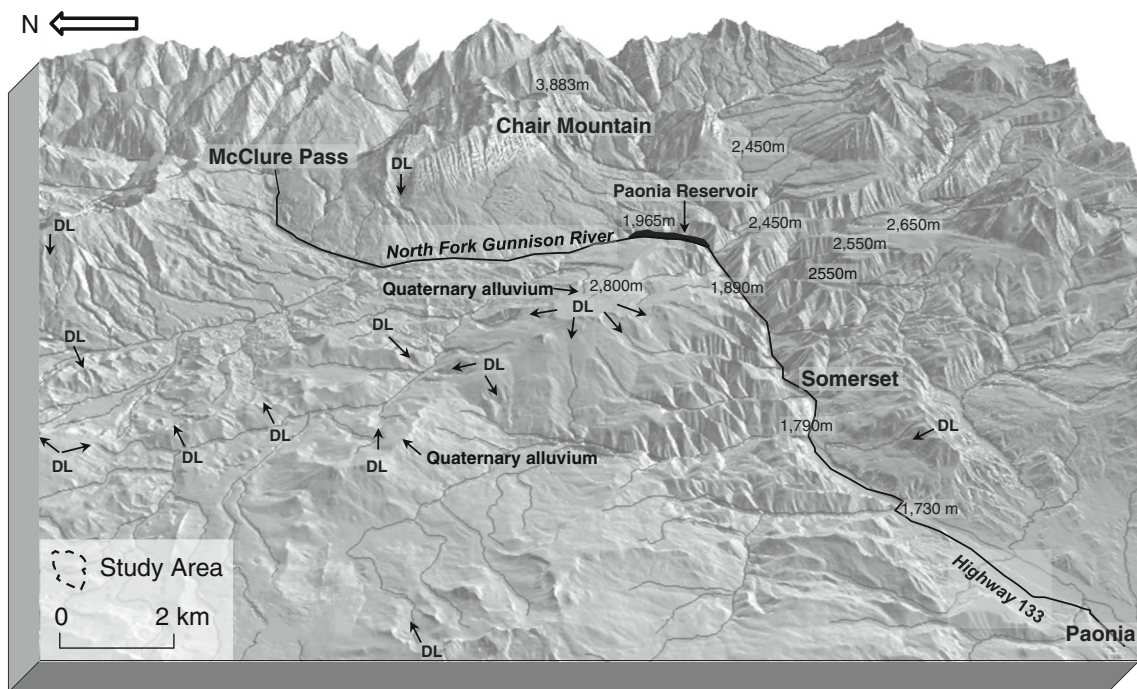


Fig. 2 A hillshaded map showing topography of the study area (figure modified after Regmi et al. 2010b). The area is composed of river floodplains and upland plateaus, steep slopes in the close proximity of the North Fork Gunnison River and associated tributaries; upland slopes is composed of large deep-seated landslides (DL) and tall and steep mountains. The elevations of the river floodplains at different locations and plateaus are shown

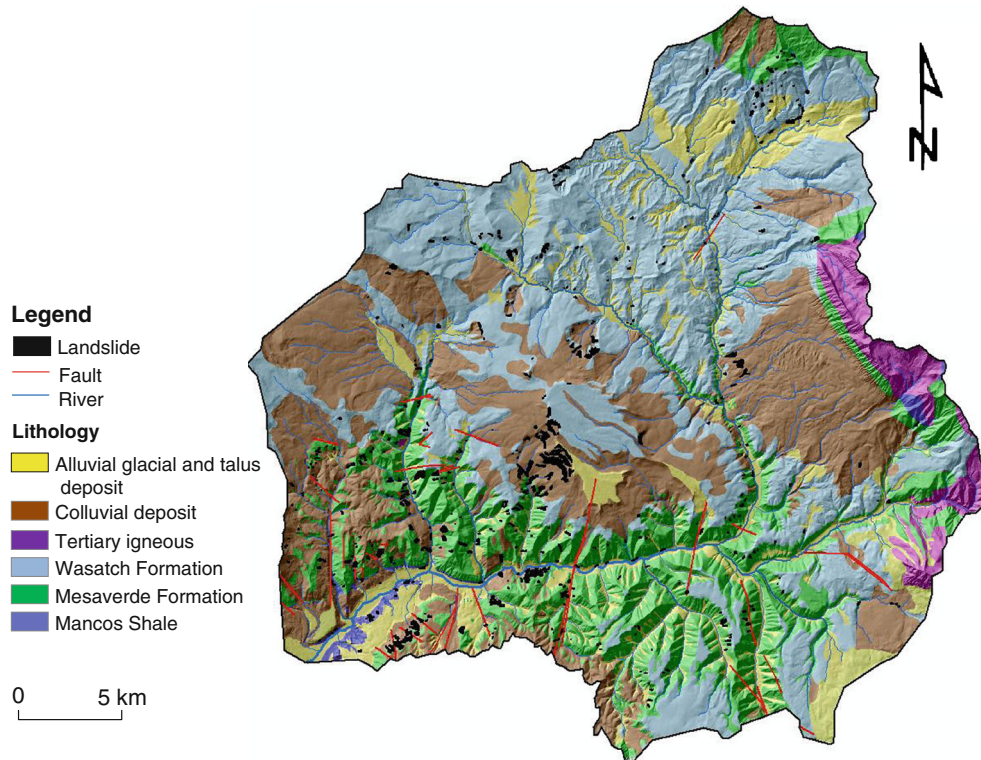


Fig. 3 A map showing shallow landslides and types of lithology present in the study area. The landslides were mapped as polygons. The area is mostly composed of alluvial, glacial, talus, and colluvial deposits of Quaternary Period. Colluvial deposits represent mostly the sediments deposited by landslides and mudflows. Major rock types in the area include: Tertiary igneous rocks; claystone, mudstone, and sandstone lenses of Tertiary Wasatch Formation; sandstone, mudstone, and shale of Upper Cretaceous Mesaverde Formation; and shale and mudstone of Upper Cretaceous Mancos Shale. A detailed lithologic description can be found in Regmi (2010) and Dunrud (1989)

under the effect of gravity and increased pore-water pressure (Fig. 6). In most of the rock and soil landslides, the boundary between the soil and the underlying bedrock is abrupt. The regolith is cohesionless, has low bulk density, and contains fragments

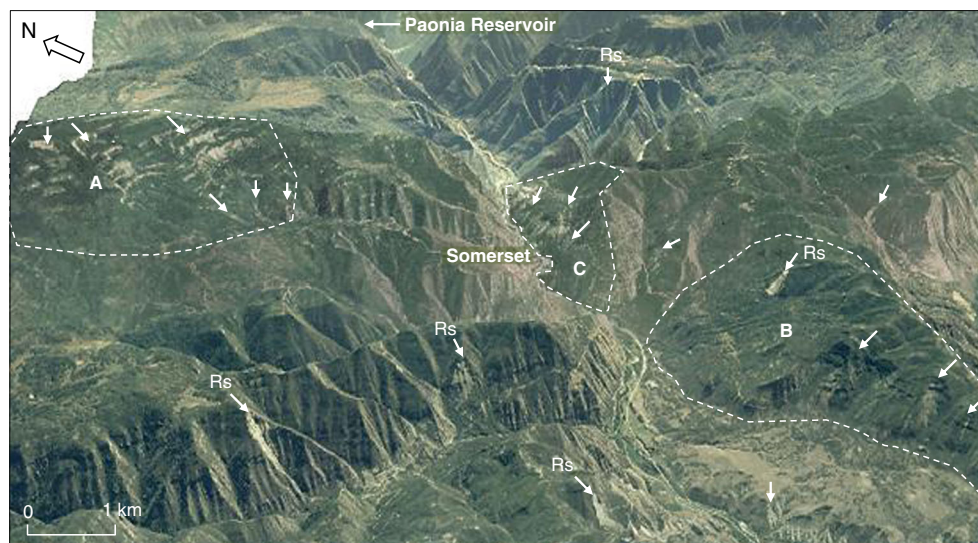


Fig. 4 Shallow and deep-seated landslides around the small community of Somerset (figure modified after Regmi et al. 2010a). The image shows a 3-D view towards the west. Rockslides (Rs) occur mostly on steep slopes. The entire hillslope, shown in zones A, B, and C, is active. Zones A and B are dominated by shallow- and deep-seated landslides. The hummocky landform in zone B and the southern slope of Somerset (zone C) are dominated by active debris flows. Only shallow landslides from these zones were mapped for the analysis. The largest river in the area flowing east–west is the North Fork of the Gunnison River; Colorado Highway 133 trends parallel to the river. The vertical scale of the image is exaggerated twice

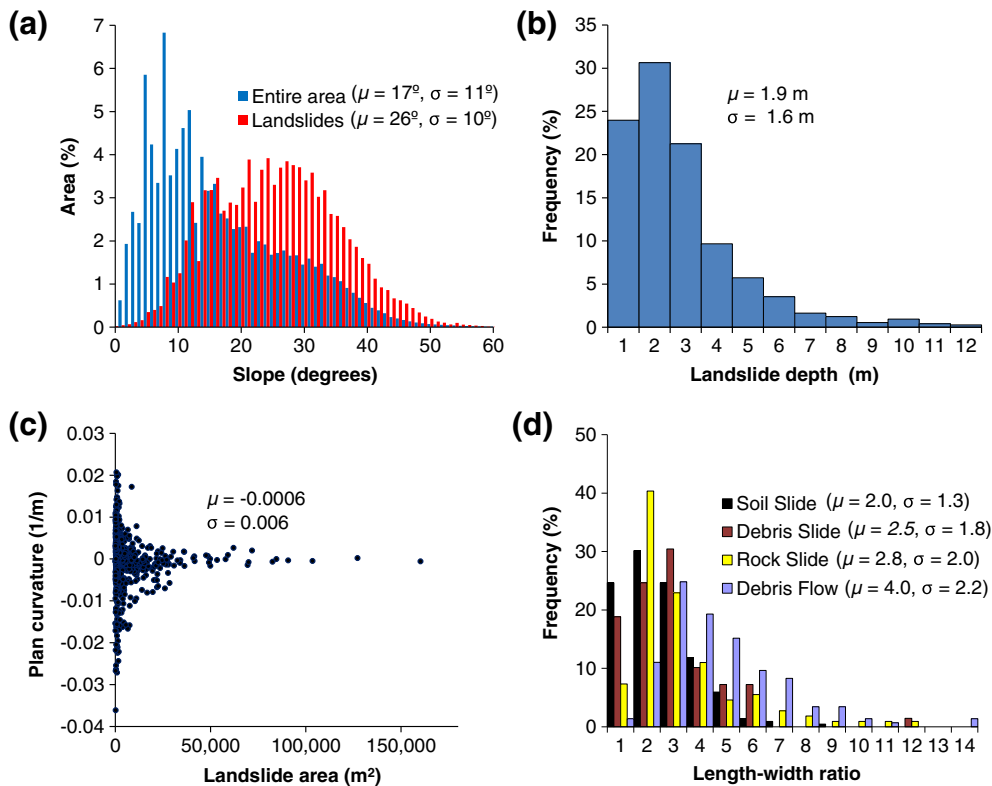


Fig. 5 Geomorphic characteristics of shallow landslides determined based on the analysis of 10 m USGS digital elevation data and 1 m NAIP aerial photographs. **a** Histograms showing distribution of the slope on the landslide surface and entire area. The average slope of the landslide surface is $\sim 26^\circ$ and entire area is $\sim 17^\circ$. **b** A histogram showing the depths of landslides. The average depth of the landslide is ~ 1.9 m. **c** A scatter plot showing areas and plan curvatures of the landslides. **d** Histograms showing runout length to width ratios of different types of landslides. μ mean, σ standard deviation

of rocks. The underlying rock is highly fractured, gently dipping and has considerable cohesion as well as frictional strength. The loose regolith conducts more water than the bedrock. Because the highly fractured underlying bedrock may conduct large amounts of water (Wilson and Dietrich 1987; Johnson and Sitar 1990; Montgomery et al. 1997), we consider that the rockslides in the area are probably the result of the rock fractures and pore-water pressure generated by subsurface flow. The main reason for the rock fractures is sufficient moisture coupled with great depth of the frost penetration in winter. Furthermore, many landslides occurred between the boundary of hard rocks (sandstone and plutonic rock) and soft rocks (mudstone and shale). An interface of differential shear strength also contributed to these landslides.

Only very limited sources describe the occurrence of shallow landslides prior to 1993. Debris flows occurred in many parts of the area during intense rainfalls in 1975, 1983, 1984, 1985, 1986, and 1987 (Rogers 2003). Based on these events and the lack of vegetation, we assumed many of the medium and small shallow landslides were initiated then. One large shallow landslide in the area has been dated back to the 1940s (Rogers 2003).

Large deep-seated landslides (paleolandslides)

We also identified and mapped locations of large deep-seated landslides ($>160,000 m^2$) from NAIP orthorectified color aerial photographs of 1:12,000 scale acquired in 2005 and USGS DEM of 10-m horizontal resolution (Figs. 2, 4 and 6). These landslides are found on

the gentle slope of higher elevations and along the edges of the upland plateaus. The surfaces of these landslides are densely vegetated and indicate the landslides are very old (probably hundreds to thousands of years). The headscarps of some of the large landslides are still active and produce shallow landslides. These landslides exhibit how shallow landslides contribute to the upslope propagation of steep edges of upland plateaus and steep heads of rivers and tributaries in the study area. The information on the large and deep-seated landslides was not included in magnitude and frequency analysis but yielded information about landscape evolution.

Materials and methods

The first objective of the study was to map landslides in the study area. Seven hundred and thirty-five shallow landslides were mapped by employing a Geographic Information System (GIS) technique on orthorectified aerial photographs of 1:12,000 scale acquired for 1993 and 2005. Landslides were identified visually by distinguishing tone, shape, size, and texture and subsequently digitized in an ArcGIS® program. Although landslides occurred as clusters in many locations, individual landslides were mapped by identifying distinct boundaries, by employing three-dimensional visualization in ArcGIS®, and stereo-visualization techniques in Terrain Navigator Pro® programs. The spatial information of landslides and attributes of area, perimeter, runout length, width, volume, type, activity, position on the hillslope, vegetation, main causes, and damage were collected from aerial photographs,

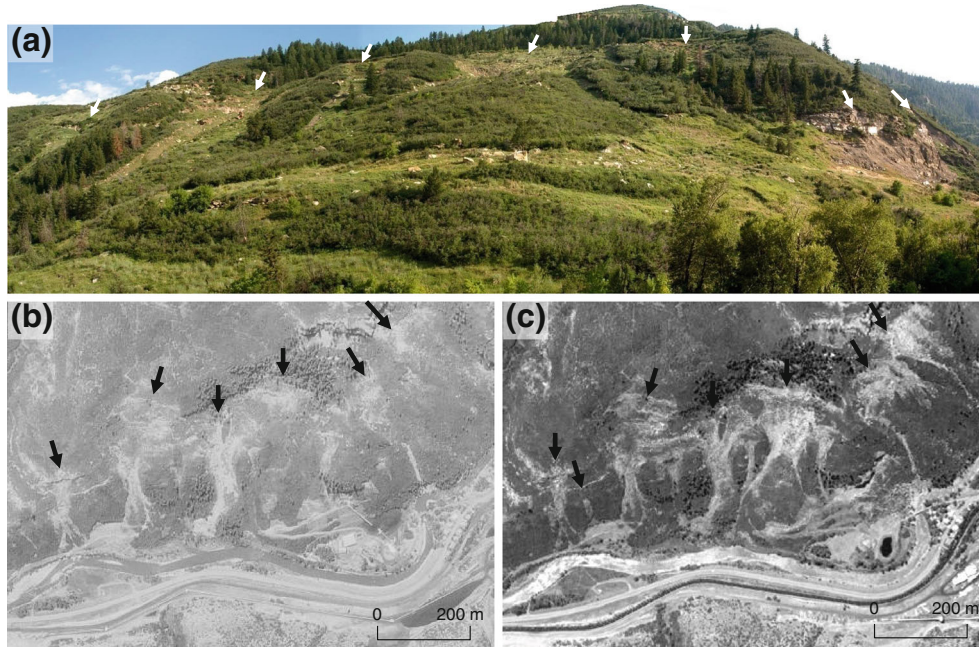


Fig. 6 Distribution of shallow landslides on the southern uphill slope of Somerset. **a** A photograph of the part of the area taken in 2006. **b** An aerial photograph acquired in 1993. **c** An aerial photograph acquired in 2005. These photographs indicate the area is quite active. Although the area has very low frequency of new landslide occurrence, the photographs show that the old landslides were reactivated and expanded during 13 years of time

historical archives and field surveys. All of these attributes were linked with spatial information from the landslides and stored in ArcGIS®. After extraction of landslide data, the location, type, and activity of all landslides were verified by field mapping.

The second objective of this study was to determine the volume of slope material displaced by each landslide. Volume, one of the important aspects in the analysis of geomorphic roles of landslides, can be used as an indicator of the magnitude of a landslide. Furthermore, additional information includes the rate of erosion/denudation, sediment yield, and the degree of hazard and risk of landslides. But, determination of accurate volumes of landslides on a regional scale is quite difficult. Researchers have used length, width, thickness or area of a landslide as a surrogate for volume. The length, width, and area of a landslide can be measured easily from aerial photographs and topographic maps. Often, however, these parameters may not provide an accurate estimation of volume. Calculation of volume from aerial photographs and topographic map is almost impossible. Volume can be determined by: (1) visual approximation in the field (Simonett 1967); and (2) analysis using a high-resolution digital elevation model (DEM) (Regmi et al. 2007). Acquiring field measurements is expensive, time consuming, and depends on the judgment of an expert. Estimating volume from a DEM can create numerous errors, from: (1) the resolution of DEM, (2) the errors in the DEM itself (Claessens et al. 2005), (3) technique used for DEM resampling, and (4) the algorithms used in the analysis (Wise 2000). Use of DEM analysis and expert's judgment based on field observation would be a better approach. The volume of each landslide was calculated by integrating the analysis of the USGS DEM with 10-m horizontal resolution and field observations. The concept behind this approach is: if an elevation surface is created by interpolating elevations of the landslide boundaries, the surface approximates the

elevation of the slope prior to the slide. When the elevation of a landslide surface is subtracted from the elevation of slope prior to the slide, the positive value of each pixel gives the depth of depletion for that pixel and the negative value gives the depth of deposit for that pixel. If the depth is multiplied by the cell size, volume of the debris moved onto that pixel and the volume of the debris moved from that pixel can be determined. The summation of the positive and negative values gives the total volume of depletion and accumulation attributable to a landslide.

The third objective of the study was to determine the probability distribution of magnitudes (area and volume) of landslides in the study area. Calculation of the probability of magnitudes for landslide has been discussed in the literature. Widely used techniques are: cumulative probability curve (e.g., Guthrie and Evans 2004a, b), logarithmic binning (Stark and Hovius 2001), derivative of cumulative frequency (e.g., Guzzetti et al. 2002), kernel density estimation (e.g., Guzzetti et al. 2008), inverse gamma distribution (e.g., Malamaud et al. 2004; Ghosh et al. 2012) and double Pareto distribution model (Stark and Hovius 2001). In this study, cumulative probability of the landslides and the probability density function (pdf) of landslide magnitudes were determined. The cumulative probability is calculated by dividing the cumulative number of landslides in descending order of their sizes by the total number of landslides. The pdf is calculated based on the Gaussian kernel density estimation method (Eq. 1) in which the estimate of the bandwidth is determined based on the Silverman's Rule of Thumb (Silverman 1984) (Eq. 2). Then the pdf was plotted against the size of the landslides and the data were fitted with a double Pareto curve. The double Pareto curve is developed based on Eqs. 3 and 4 (Stark and Hovius

2001). By using Eq. 3, data for the uniform sizes of landslides, ranging from 1 to m (the maximum size of the landslides), were simulated in which the probability (π) of the simulated sizes of landslides range from 0 to 1. Data for the sizes of simulated landslides were used in Eq. 4 to determine the probability density of given simulated sizes of landslides. The double Pareto curve is compared with the pdf curve of the real landslide data. To make a close match between these two curves, variables in the double Pareto equation as positive slope of the distribution curve (α), negative slope of the distribution curve (β), and rollover of slope (t) were changed until these curves match.

$$\hat{f}(x; h) = \frac{1}{nh^d} \sum_{i=1}^n K\left(\frac{x-x_i}{h}\right) \quad (1)$$

$$\hat{h} = 1.06 \min\left\{\hat{\sigma}, \frac{R}{1.34}\right\} n^{-1/5} \quad (2)$$

Where, \hat{f} is the density estimate, n is the number of the population, h is bandwidth, d is the dimension, x is the mean, and x_i is the value of i th population, $K((x-x_i)/h)$ is the Gaussian function, \hat{h} is the bandwidth estimate, and $\hat{\sigma}$ is the estimate of standard deviation, and R is the inter-quartile range.

$$x(\pi) = t \left\{ \pi^{-\alpha/\beta} \left[1 + \left(\frac{m}{t} \right)^{-\alpha} \right] - 1 \right\}^{-1/\alpha} \quad (3)$$

$$p(x) = \eta \left[\frac{\left[1 + \left(\frac{m}{t} \right)^{-\alpha} \right]^{\beta/\alpha}}{\left[1 + \left(\frac{x}{t} \right)^{-\alpha} \right]^{1+\beta/\alpha}} \right] \times \left(\frac{x}{t} \right)^{-\alpha-1} \quad (4)$$

Where, π =randomly selected uniformly distributed probability ranging from δ to 1, $\eta = \frac{\beta}{t(1-\delta)}$, $\delta = \pi(c)$ and c =the minimum size of the landslide.

The fourth objective of the study was to determine the sizes of the landslides which occur frequently and assess how much sediment they moved in the study area. We followed Guthrie and Evans (2007) and used magnitudes and frequencies of landslides to determine the geomorphic work performed. The logic behind this concept is based on the concept of Wolman and Miller (1960). In this approach, the frequency of landslides is considered as lognormally distributed and the geomorphic work done by a landslide of a certain size is determined by multiplying the probability or frequency and the mean magnitude or size of the given range of landslide sizes. The size of an event is determined by converting the sizes of landslides into logarithmic form and dividing the logarithmic values into equally spaced classes, as done by Wolman and Miller (1960) and Guthrie and Evans (2007). The work and the probability of landslides were plotted together with the magnitude of

landslides. This plot is used to evaluate the size range of landslides responsible for observed geomorphic work.

Results

Frequency–magnitude relationships of landslides

The relationships of the frequencies and the magnitudes of the shallow landslides were studied at two different scales. The first is the study of landslides at the local scale (Fig. 7a) and the second is the study of landslides on a regional scale (Fig. 3). Figure 7a shows the distribution of landslides, including debris flows, debris slides, soil slides, and rock slides, on two north-facing slopes near Somerset. The distribution of landslides on those slopes indicates that the sizes of landslides vary although the geomorphological and geological conditions are similar. The lower slope contains predominantly shale and the upper slope contains sandstone over mudstone. Among 31 landslides, only two landslides are relatively large landslides (20,000–83,000 m²), 11 landslides are medium-sized landslides (1,600–20,000 m²) and 18 landslides are small landslides (<1,600 m²). The probability distribution of the landslides on these slopes (Fig. 7b) shows that the probability of occurrence or the frequency for large landslides is small than compared with medium and small landslides. The probability of occurrence of landslides and the area of landslides (i.e., landslide magnitude) are related by a negative inverse power function for areas of landslides from 1,600 to 83,000 m², whereas the probability–area relationship for the landslides smaller than 1,600 m² is different.

A question regarding the frequency–magnitude relationship is: what causes the difference in the scaling power of the large and small landslides? All resolvable landslides were mapped from the photographs shown in Fig. 7a. The probability curve shows that the scaling is different for small and large landslides with rollover at $\sim 1,600$ m². The photograph (Fig. 7a) is oblique and represents a very small part of the landscape. It is possible that we could have missed some very small landslides from the upper slope, for example, the white patches indicated by the arrows without “?” symbol. Furthermore, the persistence time of smaller landslides is very low (Guthrie and Evans 2007), because the hillslope processes and vegetation modifies them very quickly. The topographic depressions shown with “?” symbols possibly are modified landslide scars. Therefore, failing to map all small landslides, a reason for the rollover effect proposed by many authors, could have played a role in the difference of power scaling. Based on our observations and the large value of t (1,600 m²) in Fig. 7b, we believe undersampling is one of the reasons for the rollover. In Fig. 7a, if the characteristics of the landslides are observed in detail, slope morphology is another factor that controls the sizes of landslides. Small landslides occur on slopes with relatively smaller slope angle and slope length. Larger landslides occur, however, on relatively steeper slopes with large slope lengths. Similarly, the size of a landslide probably depends on the curvature of the slope. Smaller landslides can be observed on slopes that have small radius of curvature or large curvature (very convex or very concave). Larger landslides occur on slopes with large radius of curvature or small curvature (nearly planar). In this regard, it can be inferred that the physical condition of slopes also influences the size of landslides.

Other possible factors that determine the size of landslides can be the characteristics of the slope material and the magnitude and frequency of triggering factors. If the characteristics of the slope

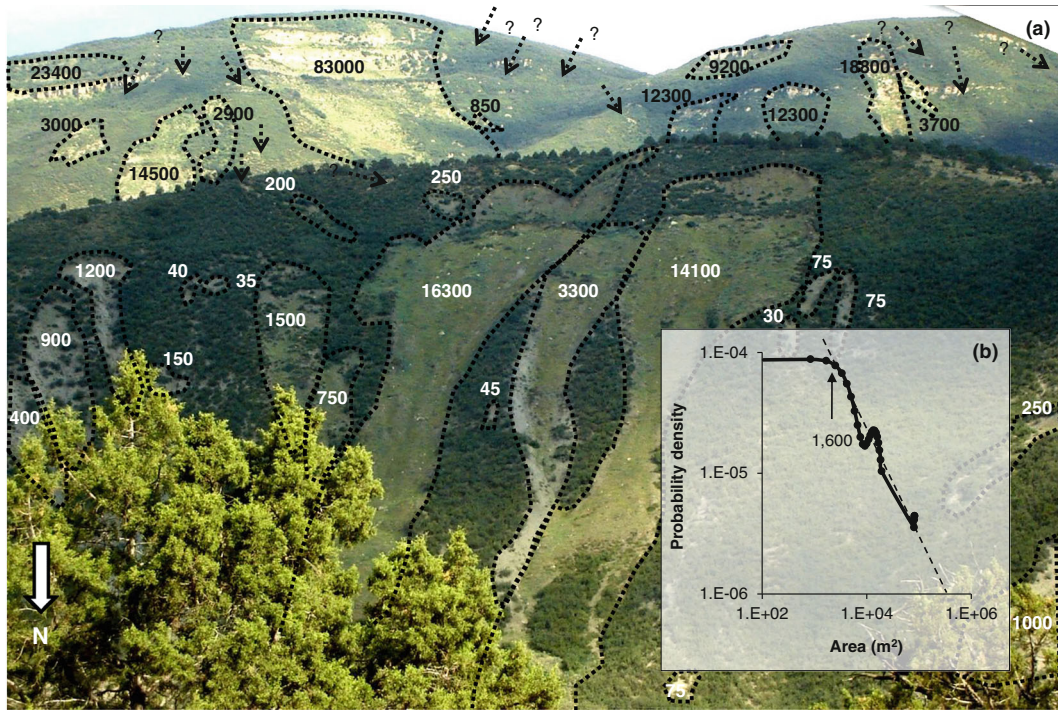


Fig. 7 Distribution of shallow landslides on a slope nearby Somerset. The area shows the variation of the size of the landslides. The *bold texts* represent the areas of the landslides in square meters. Areas indicated by *arrows with question marks* are probably landslide surfaces which were modified by the growth of the vegetation and other surface processes. Areas shown by *arrows without question mark* are landslides which are not mappable. A graph on the lower right quarter of the photographs is the plot of the probability density of the landslides with magnitudes (areas) of the landslides

material are the major reason, as described by Pelletier (1997), a question arises about the spatial variation of the soil characteristics. Evaluating the evenly distributed sizes of the landslides in each slope unit of Fig. 7a, a local area having relatively similar lithologies, provides suspicion about the sole dependency of magnitude of landslides on the characteristics of regolith (cohesive or frictional). Magnitude of a landslide is the response of the coupling effect of the spatial variability of the soil characteristics and the geometric characteristics of the slope.

Following this example we studied the distribution of the areas and volumes of 735 landslides in the region from Paonia to McClure Pass and developed frequency–magnitude curves (Fig. 8). Figure 8a shows the cumulative percentage distribution of sizes of landslides (area and volume). Figure 8b shows the plot of cumulative probability versus the sizes of landslides. Figure 8c and d show the plot of pdf versus the sizes of landslides. All curves show the rollover effect, but the curves developed by plotting pdf versus the sizes of landslides show negative power scaling for medium to large landslides and positive power scaling for small landslides separated by a rollover point. The cumulative distribution curve flattens rapidly and could be described by several relations. We observed in the field that the sizes of most landslides are controlled by the slope length, curvature of the slope, and the characteristics of the materials. The change in the slope profile from steeper to gentle slopes causes most of the landslides to stop on the slope and immediately deposit the displaced material. Many landslides ended in the rivers and on roads. Zones of convergence are the sites of the frictional regolith where most of

the medium- and large-sized debris flows and debris slides occur. Large rockslides and debris slides occur on nearly planar slopes having shattered rocks and frictional regolith. Soil slides, mostly small events, occur on all kinds of slope curvatures (convex, concave, and planar) with soils of slightly cohesive nature.

Figure 8c, d shows that the double Pareto models fit well with the probability distribution curves for the areas and volumes of landslides. The probability curve for landslide area rolls at $t=1,600 \text{ m}^2$, with power scaling for large and medium landslides as $\alpha=1.1$ and for small landslides as $\beta=1.9$. The probability plot for landslide volume rolls at $1,900 \text{ m}^3$ with the power scaling value for large and medium landslides as $\alpha=1.15$ and the scaling for smaller landslides as $\beta=1.9$. Both curves show similar trends of power scaling. A small value of α and a large value of β indicate that the distribution has a long tail, which means the mass movement process in the area is debris dominated. Although 328 landslides have an area less than the area at rollover point ($1,600 \text{ m}^2$), the total area of these landslides is only 6 % of the total area of all landslides and the total volume of the material displaced by these landslides is only 1.5 % of the total volume of debris mobilized by all landslides (Fig. 8a). This indicates that the slope material mobilized by small landslides is very insignificant in comparison to the amount of slope material mobilized by medium and large landslides.

Area–volume relationship of shallow landslides

Precise or even approximate calculation of the volume of landslides is quite difficult in the study area. Mountainous regions of western Colorado are densely forested and often inaccessible. The best way to estimate the volumes of landslides is by the analysis of aerial

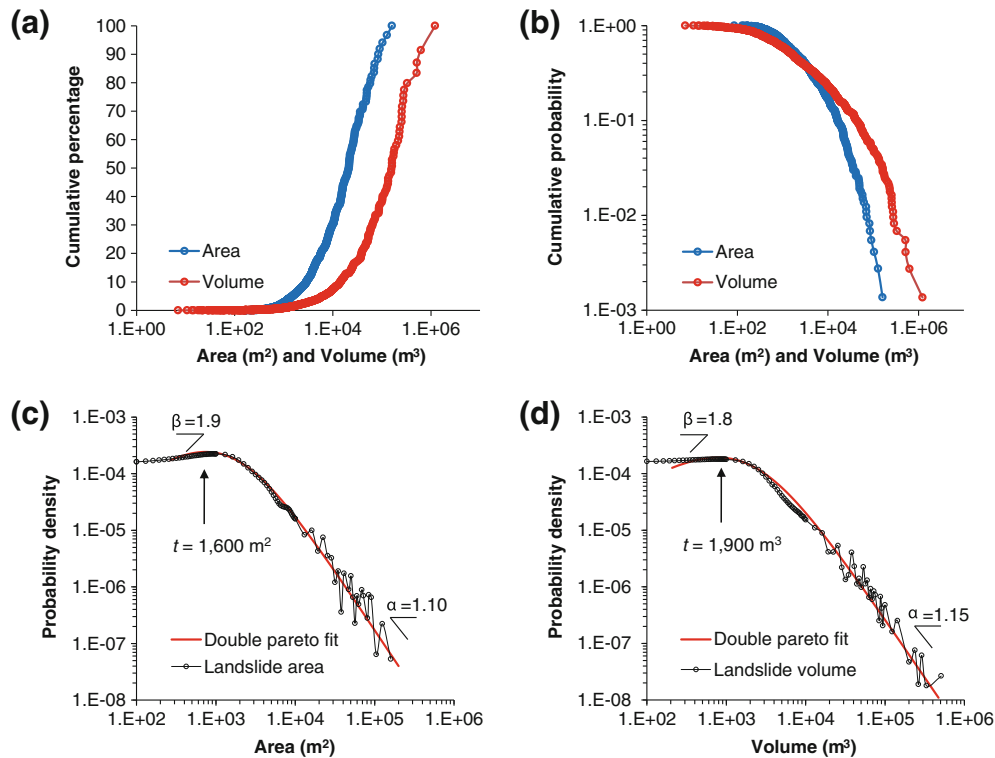


Fig. 8 Figures showing frequency–magnitude relationships of shallow landslides. The frequency is defined as: **a** cumulative percentage of landslide areas and volumes, **b** cumulative probability of landslide areas and volumes, **c** probability density of landslide areas, and **d** probability density of landslide volumes. The slopes of the relationship curves (**c**, **d**) were determined based on the comparison with fitted double Pareto curves

photographs and DEMs. Similar to the other studies, this study shows that the areas and the volumes of landslides are related by a power relationship (Table 1 and Fig. 9). An empirical equation was obtained (Eq. 5) to estimate the volumes of landslides based on the least square regression ($R^2=0.87$) of areas (A) and the estimated volumes (V) of 735 landslides.

$$V = 0.0254 \times A^{1.45} \quad (5)$$

The area–volume relationships of landslides described in six articles (Table 1) are compared with our results (Fig. 9b). The result is not significantly different from Hovius et al. (1997), Guzzetti et al. (2008), Innes (1983), and Simonett (1967), whereas the result is significantly different than those obtained by Korup

(2005) and Guthrie and Evans (2004a) (Table 1 and Fig. 9b). The equation obtained by Korup (2005) is for very large landslides ($A > 1 \text{ km}^2$) and may be the reason for results different than this study.

The areas of recorded landslides ranged from 85 to $1.6 \times 10^5 \text{ m}^2$. The total area eroded by all landslides is $4.8 \times 10^6 \text{ m}^2$ with the average area of $6,600 \text{ m}^2$ and a standard deviation of $1.36 \times 10^4 \text{ m}^2$. The average thickness of the landslides studied is 1.9 m, and the total volume of the soil displaced by all landslides is $1.4 \times 10^7 \text{ m}^3$ with the average volume of $20,000 \text{ m}^3$ and standard deviation of $7 \times 10^4 \text{ m}^3$. This is a lower estimate of the total volume of landslides because only distinguishable landslides were considered in the analysis. Only 36 landslides have a volume larger than $1 \times 10^5 \text{ m}^3$, and these landslides contribute 62 % of the total volume of all landslides. The three largest landslides (landslide area, 1×10^5 – $1.6 \times 10^5 \text{ m}^2$) mapped in the area

Table 1 Comparison of the landslide volumes and areas with the results obtained by many researchers around the world

Equation	Landslide area range (m^2)	Source	Area of study	Mean volume (m^3)	Landslide type
$V=0.0254 \times A^{1.45}$	85– 1.6×10^5	This study	Western Colorado	2×10^4	Shallow
$V=0.0844 \times A^{1.43}$	170– 5.5×10^6	Guzzetti et al. (2008)	Central Italy	3.9×10^5	Shallow and large
$V=0.024 \times A^{1.36}$	NA	Simonett (1967)	Central Italy	3.2×10^5	Shallow and large
$V=0.05 \times A^{1.5}$	100– 1×10^6	Hovius et al. (1997)	Central Italy	5.4×10^5	Shallow and large
$V=0.02 \times A^{1.95}$	5×10^4 – 5×10^6	Korup (2005)	Central Italy	1.43×10^5	Large
$V=0.0329 \times A^{1.39}$	30–900	Innes (1983)	Scottish Highlands	NA	Shallow
$V=0.1549 \times A^{1.09}$	1,124– 4.09×10^6	Guthrie and Evans (2004a, b)	British Columbia	NA	Shallow and large

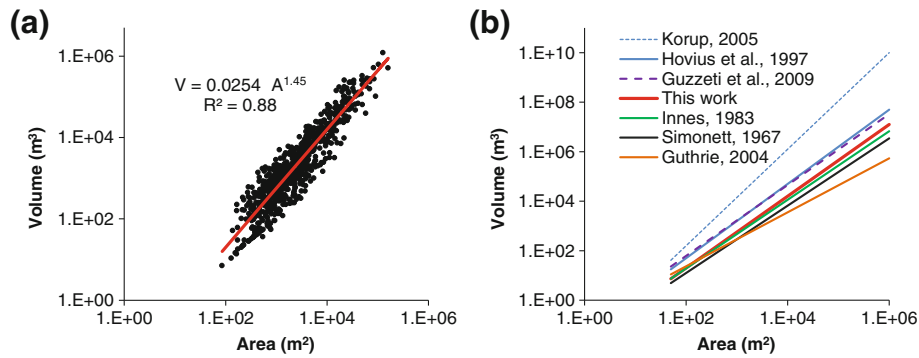


Fig. 9 Figures showing volume-area relationships of shallow landslides: **a** the relationship from the present study and **b** its comparison with the results obtained by many researchers around the world

(~0.4 % of total number) account for ~17 % of the total landslide volume; 58 landslides (landslide area, 20,000– 1×10^5 m²) mapped in the area (~8 % of total number) account for ~54 % of the total landslide volume; 346 landslides (landslide area 1,600–20,000 m²) mapped in the area (~47 % of total number) account for 28 % of the total landslide volume and 328 landslides (landslide area 85–1,600 m²) mapped in the area (~44 % of total number) account for ~1.4 % of the total landslide volume. These data confirm the importance of large landslides in determining the total volume of landslide material in the study area.

The geomorphic work performed by the shallow landslides of different sizes

The probability and work curves indicate that smaller landslides have higher probability of occurrence and do less work whereas larger landslides have lower probability of occurrence and perform more work (Fig. 10). These curves show that the size of a landslide ~1,600 m² (3.2 in log₁₀ value) has the highest probability of occurrence but the landslide size ~20,000 m² (4.3 in log₁₀ value) creates the most work. A range of sizes of landslides which have high probability and high work are the important landslides for geomorphic effectiveness. This means the landslides with the range of sizes lying between these two peaks have potential roles in creating significant geomorphic change from sediment yield in Paonia–McClure Pass area. About 226 landslides are found within the area range of 1,600 to 20,000 m². These landslides, the medium-sized landslides, mobilized about 30 % of the total volume attributed to landslides.

Spatial distribution of shallow landslides and sediment yield

In addition to the magnitude, the spatial distribution of landslides also describes the role of landslides in the evolution of a landscape. Unstable areas of a landscape tend to have a cluster of landslides. Landslides in the study area are not distributed uniformly. They are clustered in 60 regions among which only eight zones are major (Fig. 11). Major areas of the landslides are A to H in Fig. 11. Shallow landslides in zones A and B are influenced by the deep-seated landslides. The flow structures and the shape of landslides defined by large values of length/width ratio in zones C, D, E, and G indicate that the landslides were triggered either by intense rainstorms or by extensive snowmelt. Landslides in zone F are related to the weathered and highly fractured rocks. Landslides in zone H occur in colluvium, glacial till and highly weathered rocks.

The maximum density of landslide is 13 landslides/km² (Fig. 11a). In terms of the area, the maximum density of a landslide is 0.347 sq. km of landslide area per square kilometer of the study area (Fig. 11b). Similarly, maximum volume of material displaced is 1.3×10^6 m³ from 1 square kilometer of the study area (Fig. 11c).

A map showing the standard deviation of the elevation (SDE) for each pixel within the circle of 100 m diameter implies that the geomorphic expression of the area can be differentiated into four categories (Fig. 12). Zone I is the area of low relief variability (SDE=0–2 m) and is composed of river floodplains and upland plateaus. Zone II is the rough and steep zone in close proximity to the streams and is defined by a contributing area of >10 km² (SDE=5–20 m). The slopes of the zone result from river incision, erosion and toe cutting of the slopes. Most of the shallow landslides in the study area occur in this zone. The geology of the zone II is sandstone and mudstone that are highly fractured and weathered. The average slope of this zone is $25.6 \pm 11^\circ$, whereas the average slope of the entire study area is $17 \pm 11^\circ$. This indicates that many of the slopes within zone II are more unstable than the slopes of other areas. Zone III, the upland gentle slope (SDE=2–5 m), contributes to deep-seated large landslides. Shallow landslides also occur on the headscarps of the deep-seated large landslides in this zone. Zone IV is the steep slopes formed by the rocks and the tall mountains developed by the igneous intrusions (SDE=>20 m). Rock glaciers, horns, and arêtes are the characteristic

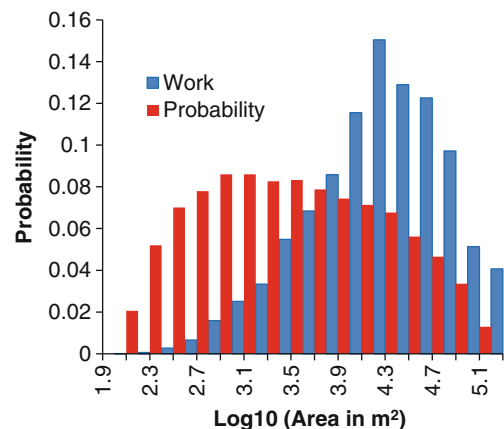


Fig. 10 Histograms showing the probability distribution of the landslide areas in logarithmic intervals and the work performed by the landslides of each logarithmic interval. Work is defined as probability \times Area and then scaled to fit the graph

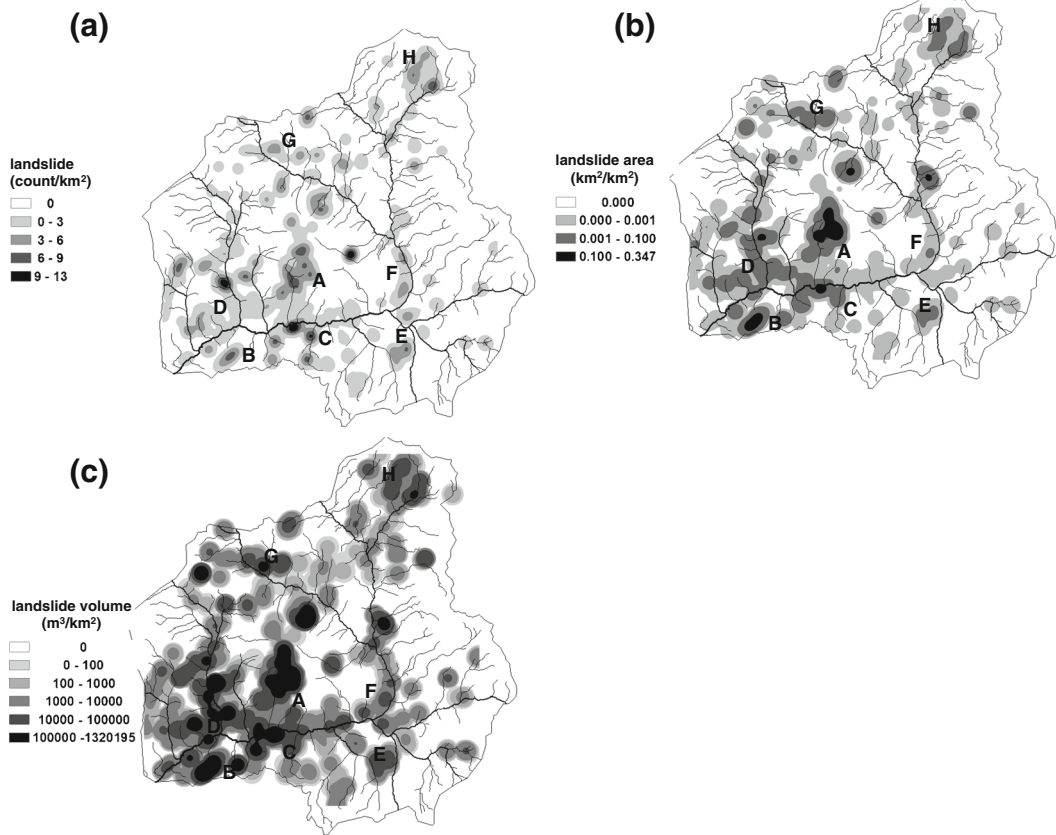


Fig. 11 Spatial density of shallow landslides computed in terms of: **a** count, **b** area, and **c** volume of the landslides per square kilometer of the area. The density maps were developed based on the kernel density estimation of each landslide attribute within 1 km² circular neighborhood. Note that all the density maps show clustering of landslides in 60 clusters, and among them, eight (A–H) are considered major

landforms of this zone. Figure 12a, b shows that a relief variability map alone can be used to predict the landslides in the area with 75 % accuracy because most of the shallow landslides in the study area occurred on steep slopes in close proximity to the rivers and associated tributaries. Most of the small- and medium-sized debris flows occurred on the convergent zones of the first-order tributaries whereas rock slides and debris slides occurred on the nearly planar steep slopes.

The ages of the shallow landslides were estimated based on the oldest landslides recorded by Colorado Geological Survey and empirical equations developed by Guthrie and Evans (2007). The oldest landslide recorded by the Colorado Geological Survey occurred in 1940. Based on the equations of the persistence time for debris slides and debris flows ($PDS = 2.5834 \times A^{0.3248}$) and rock slides and rock avalanches ($PRS = 6 \times 10^{-5} \times A^{1.2631}$), the age of the largest debris flow (155,000 m²) in the study area is obtained as

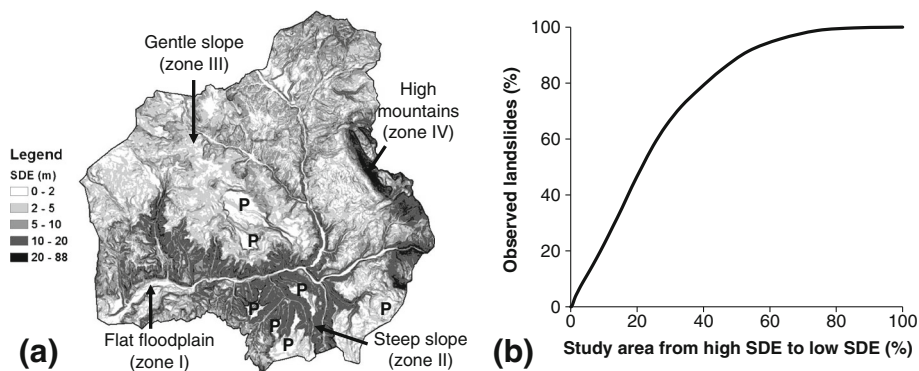


Fig. 12 **a** A map showing the standard deviation of the elevation (SDE) within a roving circular window of 100 m, and **b** a graph suggesting that the SDE map is quite effective in predicting existing landslides with 75 % of prediction accuracy (0.75 area under the curve)

125 years old and the largest rock slide (160,000 m²) is obtained as 225 years old. Only three landslides are larger than 100,000 m². These landslides account for the 17 % of the total landslide volume. If we ignore these landslides in the calculation of the rate of denudation contributed by the landslides, the largest rockslide has 70,000 m² (~ 80 years old) area and the largest debris slide is 90,000 m² (~105 years old) area. We ignored the largest three landslides from the analysis and roughly estimated that the oldest landslide in the study area is ~100 years old. The shallow landslides that occurred before this period were either modified by the surface processes or covered by dense vegetation.

Based on this estimation of the age of landslides, the volume of the soil displaced by landslides each year is $\sim 1.2 \times 10^5$ m³ and the contribution of shallow landslides to the rate of denudation for the entire area (815 km²) is at least ~ 0.15 mm year⁻¹. The calculated overall rate of denudation yields a very rough estimate based on a number of assumptions: (1) each year the same number of landslides occurred, which is not true, because most of the rainstorm influenced landslides occurred during 1980s and only 35 landslides occurred after 1993; (2) the landslides are distributed uniformly within the study area, which is also false because landslides are clustered in many locations; (3) all landslides were not mapped because of the scale of the study and modification of some landslides by vegetation and erosional processes; and (4) the time span of the studied landslides is a rough estimate which based on a generalized equation proposed by Guthrie and Evans (2007). However, the comparison of this result with the published rate of hillslope denudation in many tectonically active terrains of the world (Lave and Burbank 2004; Roering et al. 2007; Palumbo et al. 2011) suggests that the result obtained in this study seems acceptable to explain the response of mass movement in a mountainous area of western Colorado that is not very active tectonically.

As mentioned above, the approximated rate of denudation in the entire area is 0.15 mm year⁻¹. Whereas most of the landslides occur in zone II, and the rate of denudation from this zone is 0.20 mm year⁻¹. This also suggests that zone II is very unstable in comparison to the other areas.

Contribution of landslides to the landscape evolution

In addition to the frequency–magnitude relationship, geomorphic work, and sediment yield of landslides, this study briefly describes the evolution of the landscape in the study area from incision of the North Fork of Gunnison River and associated streams and the contribution of shallow and deep-seated landslides in the appearance of the landscape. Fluvial geomorphology in western Colorado is largely characterized by climatically controlled cycles of aggradation and incision (Darling et al. 2009). Cycles of aggradation and incision are generally linked to the glacial and interglacial oscillations (Sinnock 1981; Dethier 2001; Sharp et al. 2003) and result in a series of terraces. Older terraces are higher in elevation than younger terraces (Bull 1991). The study area, composed of many upland plateaus, shows relict topography of the Quaternary Period. Some of the plateaus exhibit Quaternary fluvial deposits (probably the deposits of the ancient Colorado River). The total relief of one of the plateaus near Somerset, with respect to the nearest point at the North Fork of Gunnison River, is ~800 m which indicates that the river incised at least 800 m during the Quaternary period and the response of the incision is zone II type of geomorphic form. The rate of incision of the Gunnison River, based on the study at and around the Black Canyon of Gunnison and Unaweep Canyon in western

Colorado, varies from 61 to 142 m/Ma (Aslan et al. 2008). Similarly, the study assessed the incision of the Gunnison River as ~1,550 m based on the elevation of the 10 Ma old basalt capped Grand Mesa (Fig. 1) and Delta which indicates that the rate of incision of the Gunnison River is at least 155 m/Ma.

Based on the field observations of landslides and the history of incision by rivers in the study area, we developed a simple conceptual model of the landscape evolution contributed by the incision and toe cutting of the North Fork Gunnison River and associated tributaries, shallow landslides and the deep-seated landslides (Fig. 13). Although the present slopes around the rivers and tributaries of the study area are not perfectly symmetrical, as shown in Fig. 13, the sketches present a concept of how the landscape was modified during the Quaternary to the present time. It is hypothesized that during Quaternary Period the topography of the area was very gentle with large plateaus most probably developed by the incisional and aggradational nature of Ancient Colorado River (?) from Early Miocene to the Quaternary time (Epis et al. 1980). This concept is supported by a 10 Ma basalt flow and the existence of ancient fluvial deposits capping many plateaus (e.g., Grand Mesa) around the study area. The first figure (Fig. 13a) shows the beginning of the river incision into a large region of upland plateau. The second figure (Fig. 13b) shows river incision in close proximity to steep slopes ($S_{B2} > S_{B1}$) because of the base level being lowered. These slopes also tend to be stabilized by shallow landslides. The upslope regions change to a more unstable condition because of the increasing energy ($\text{energy} = mgh_2$) on steeper slopes. The shallow landslides are a process–response reaction to river incision and frequent toe cutting. With continuous lowering of the base level, the area develops two distinct slopes ($S_{C2} > S_{C1}$) and the relief of the upland plateaus increases ($h_3 > h_2$) (Fig. 13c). The steep slopes retreat as shallow landslides occur and the upland slopes reach an instability threshold because of the high energy (mgh_3). Because incision processes are continuous, the high levels of energy present in the uplands exceeds ($mgh_1 < mgh_2 < mgh_3$) the instability threshold. Under the effect of the gravity, deep-seated large landslides are produced (Fig. 13d). These deep-seated landslides steepen the upland gentle slope by propagating upslope (Fig. 13e) and form three types of slopes ($S_{E1} > S_{E2} < S_{E3}$). Figure 13e is similar to the topographic profile of the recent topography nearby Somerset and areas around the center of the study area. Although the large deep-seated landslides (paleolandslides) were not introduced in the frequency–magnitude analysis, we presumed that the frequency of the shallow landslides is larger than the frequency of deep-seated large landslides. The dense vegetation on the surface of the deep-seated landslides also suggests that the frequency of these landslides is very small in comparison to the frequency of shallow landslides. No deep-seated large landslides occur on some of the plateaus in the study areas (e.g., upper right center of Fig. 2). Low relief and hard rock lithology, i.e., sandstone and mudstone, contribute to this condition. In contrast, this model supports deep-seated large landslides along the edges of the Grand Mesa and other mesas having relatively high relief.

The geology of the study area also plays a major role in the present physiographic expression of the area. Zone II is composed of fractured and weathered sandstone and mudstone, whereas zone III is underlined by thick colluvium and glacial till.

Discussion and conclusions

Seven hundred and thirty-five shallow landslides were analyzed to evaluate the frequency–magnitude relationship and geomorphic

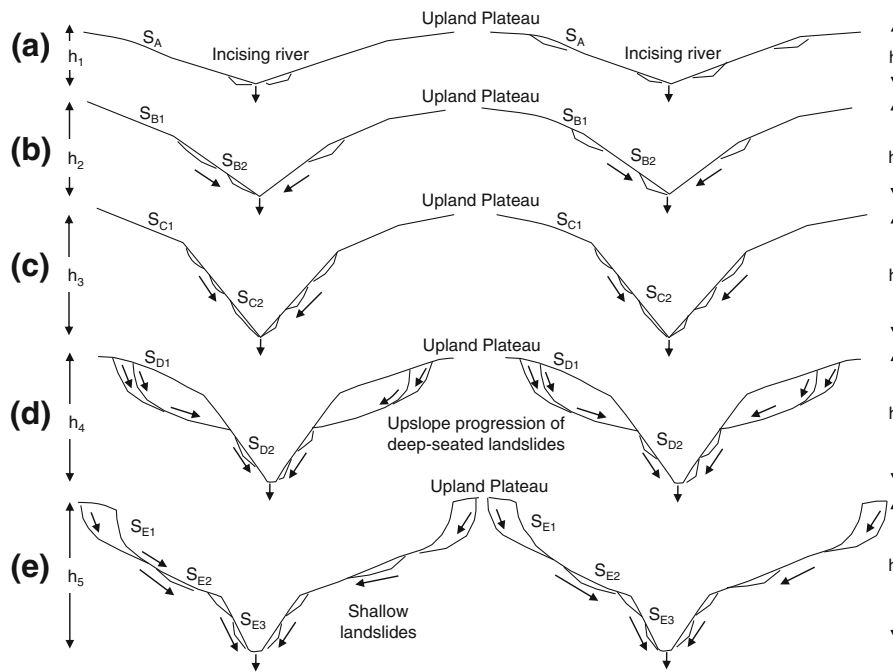


Fig. 13 A simple model of landscape evolution in Paonia–McClure Pass area. Although the present slopes in the area around the rivers and tributaries are not perfectly symmetrical as shown in the figure, the sketches present a concept of how the landscape in the area was modified over time from Quaternary to present. **a** Figure shows the beginning of the river incision with a large region of upland plateau. **b** As rivers undergo incision, the regions in close proximity to the rivers develop steep slopes and the slopes tend to stabilize by the shallow landslides. **c** The relief of the upland plateaus increases ($h_3 > h_2$) with two distinct slopes ($S_{C2} > S_{C1}$). The steep slopes retreats by the shallow landslides, and the upland slopes reach to the instability threshold because of the high potential energy. **d** Because the incision processes are continuous, the high potential energy upland exceeds the instability threshold and under the effect of the gravity produces deep-seated large landslides. **e** These deep-seated landslides steepened the upland gentle slope by propagating upslope. The recent condition of the topography nearby Somerset is shown in (e)

work of landslides. These landslides were mapped on aerial photographs acquired in 1993 and 2005. Seven hundred landslides were identified on the aerial photographs from 1993 and 35 more landslides were identified on the aerial photographs acquired in 2005. Many landslides were reactivated between 1993 and 2005 (e.g., Fig. 6). The slope varies with the lithology. Most of the medium to gentle slopes are observed in mudstone and shale whereas steep slopes are observed in sandstone and intrusive rocks. The distribution of the slope angles of the landslide surfaces is different than the distribution of slopes in the total area (Fig. 5). Slope zone 10–20° is dominant in the entire area whereas slope zone 20–30° is dominant on landslide surfaces. Most of the landslides were observed on slopes ranging from 15–40° with mean value of 26°. Many of the landslide scars connect to the sediment deposited at the toe. The total volume deposited for all landslides, however, is lower than the total volume transported, which indicates that the sediments were washed down the slope. The ratio of the mass moved down slope to the mass accumulated on the toe of landslides for small landslides is less than for large landslides.

All curves of probability and magnitude of landslides show a rollover effect. The double Pareto model of the relationship of landslide frequency and magnitude (landslide area) shows that the value of power law scaling for larger landslides is $\alpha=1.12$ and power law scaling for smaller landslides is $\beta=1.90$ and the rollover in slopes of power curves is a $t=1,600 \text{ m}^2$ (Fig. 8c). Similarly, values of these parameters for volume of mass moved as magnitudes of landslides are: $\alpha=1.15$, $\beta=1.80$, and $t=1.900 \text{ m}^3$ (Fig. 8d). In both cases, values of power law scaling parameters are quite similar.

These values along with the relationship of areas and volumes of landslides (Fig. 9), first indicate that the calculation of volume is acceptable. Second, the curves with high values of the scaling for smaller and relatively low values of power scaling for larger landslides indicate that the movement of the mass is dominated by debris rather than erosion. The methodology used to determine the volume is appropriate for medium-sized landslides but is inappropriate for very small and very large landslides. The prior slope of these landslides may not be smooth and the resolution of DEM is not sufficient to detect the signature of very small landslides. Furthermore, if the landslide surface is reactivated, the method gives the volume transported for the history of the slide. This problem was corrected based on the field observation of landslide volumes. Landslide area and depleted volume are also related by power function (Fig. 9). The result is consistent and not significantly different from the result determined in other studies around the world (Table 1).

Landslides contributing major amounts of work for the geomorphic effectiveness in the area are mostly medium landslides (size ranging from 1,600 to 20,000 m^2) which have medium probability of occurrence (0.6–0.8) or medium frequency (Fig. 10). Landslides falling within this range have higher probability and perform more work compared to landslides of other sizes. The total volume displaced by the landslides is $1.4 \times 10^7 \text{ m}^3$. The average rate of denudation of the hillslope is $0.15 \text{ mm year}^{-1}$. This amount is based on the volume of the soil mass displaced by 732 landslides (3 landslides out of 735 landslides were believed to have ages >100 years). Although only 732 landslides were observed in the last 100 years, this total cannot be true. The study failed to identify many landslides which occurred in this time

period because the landslides were either modified by the surface processes or covered by the dense vegetation so that the signature of these landslides on aerial photographs and a DEM is not extractable. Therefore, the rate of denudation should be higher than the observed value.

First, comparison of the equation for area-volume relationships of landslides with the equations obtained by others suggests that the approach used to calculate volume for landslides is valid. Second, the double Pareto relationship of frequencies and magnitudes of landslides in Paonia–McClure Pass area indicates that the mass movement in the area is debris dominated. Although the frequency of the landslides is low (732 landslides in ~100 years or ~7 landslides in a year on average), they produce debris that is fluxed into the rivers. Landslides of sizes ranging from 1,600 to 20,000 m² are the most hazardous because they occur frequently and play a major role in the modification or evolution of landscape.

The model describing the contribution of landslides to the evolution of landscapes in Paonia–McClure Pass area is supported by the location of the observed deep-seated landslides, observed and predicted shallow landslides, and the landslides doing much of the geomorphic work. Most of the deep-seated landslides are located on the circumference of the upland plateau. The observed and predicted shallow landslides as well as shallow landslides doing much of the geomorphic work are found on the steep slopes in close proximity to the rivers and tributaries, slopes of inner gorges and heads of the first-order streams as well as circumference of the plateaus. The characteristics of these landslides demonstrate how landslides contribute to the conversion of a large plateau or mesa into a rugged mountainous topography by upslope propagation of steep slopes. Furthermore, these landslides are well clustered and indicate areas that are currently unstable. Toward the center of the study area, landslides cluster on the slopes of inner gorges around a plateau. Evidence suggests that the landscapes evolve by river incision and the dominance of the low frequency deep-seated large landslides towards the upper portion of the slopes whereas the middle and the lower portion of the slopes tend to reach stabilization by frequent shallow landslides.

References

- Anderson RS (1994) Evolution of the Santa-Cruz Mountains, California, through tectonic growth and geomorphic decay. *J Geophys Res Solid Earth* 99:20161–20179
- Aslan A, Karlstrom K, Hood W, Cole RD, Oesleby T, Betton C, Sandoval M, Darling A, Kelley S, Hudson A, Kaproth B, Schoepfer S, Benange M, Landman, R (2008) River incision histories of the Black Canyon of the Gunnison and Unaweep Canyon: interplay between late Cenozoic tectonism climate change, and drainage integration in the western Rocky Mountains. In: Reynolds RG (ed.) *Roaming the rocky mountains and environs: geological field trips*. Geological Society of America Field Guide 10. The Geological Society of America, Boulder pp. 175–202
- Brardinoni F, Church M (2004) Representing the landslide magnitude-frequency relation: Capilano River Basin, British Columbia. *Earth Surf Process Landforms* 29:115–124
- Brardinoni F, Slaymakerl O, Hassan MA (2003) Landslide inventory in a rugged forested watershed: a comparison between air-photo and field survey data. *Geomorphology* 54:179–196
- Bull WB (1991) *Geomorphic responses to climate change*. Oxford University Press, New York, 326 pp
- Burbank DW, Leland J, Fielding E, Anderson RS, Brozovic N, Reid MR, Duncan C (1996) Bedrock incision, rock uplift and threshold hillslopes in the northwestern Himalayas. *Nature* 379:505–510
- Burton A, Bathurst JC (1998) Physically based modeling of shallow landslide sediment yield at a catchment scale. *Environ Geol* 35:89–99
- Cardinali M et al (2002) A geomorphologic approach to estimate landslide hazard and risk in urban and rural areas in Umbria, central Italy. *NHESS* 2:57–72
- Claessens L, Heuvelink GBM, Schoorl JM, Veldkamp A (2005) DEM resolution effects on shallow landslide hazard and soil redistribution modeling. *Earth Surf Process Landforms* 30:461–477
- Corominas J, Copons R, Vilaplana JM, Altimir J, Amigo J (2003) Integrated landslide susceptibility analysis and hazard assessment in the principality of Andorra. *Nat Hazard* 30:421–435
- Crozier MJ (1999) Prediction of rainfall-triggered landslides: a test of the antecedent water status model. *Earth Surf Process Landforms* 24:825–833
- Crozier MJ, Glade T (1999) Frequency and magnitude of landsliding: fundamental research issues. *Z Geomorphol Suppl* 115:141–155
- Dai FC, Lee CF (2001) Frequency–volume relation and prediction of rainfall-induced landslides. *Eng Geol* 59:253–266
- Darling AL, Karlstrom KE, Aslan A, Cole R, Betton C, Wan E (2009) Quaternary incision rates and drainage evolution of the Uncompaghere and Gunnison Rivers, western Colorado, as calibrated by the Lava Creek B ash. *Rocky Mt Geol* 44:71–83
- Delgado J, Pelaez JA, Tomas R, Garcia-Tortosa FJ, Alfaro P, Casado L (2011) Seismically-induced landslides in the Betic Cordillera (S Spain). *Soil Dyn Earthq Eng* 31:1203–1211
- Dethier P (2001) Pleistocene rates in the western United States calibrated using Lava Creek B tephra. *Geology* 29:783–786
- Dunrud RC (1989) Geologic map and coal stratigraphic framework of the Paonia area, Delta and Gunnison counties, Colorado. U.S. Geological Survey, Coal Investigations Map C-115, scale 1:50,000
- Epis RC, Scott GR, Taylor RB, Chapin CE (1980) Summary of Cenozoic geomorphic, volcanic, and tectonic features of central Colorado and adjoining areas. In: Kent HC, Porter KW (eds) *Colorado geology: Denver, Colorado*. Rocky Mountain Association of Geologists, Denver, pp 135–156
- Evans SG (2003) Characterizing landslide risk in Canada. 3rd Canadian Conference on Geotechnique and Natural Hazards. Canadian Geotechnical Society, Edmonton, Canada, pp 35–50
- Fujii Y (1969) Frequency distribution of landslides caused by heavy rainfall. *J Seismol Soc Jpn* 22:244–247
- Gerrard J (1994) The landslide hazard in the Himalayas: geological control and human action. Elsevier, Amsterdam. pp. 221–230
- Ghosh S, van Westen C, Carranza EJM, Jetten VG, Cardinali M, Rossi M, Guzzetti F (2012) Generating event-based landslide maps in a data-scarce Himalayan environment for estimating temporal and magnitude probabilities. *Eng Geol* 128:49–62
- Glade T (2003) Landslide occurrence as a response to land use change: a review of evidence from New Zealand. *Catena* 51:297–314
- Greenbaum D, Tutton M, Bowker M, Browne T, Buleka J, Greally K, Kuna G, McDonald A, Marsh S, O'Connor E, Tragheim D (1995) Rapid methods of landslide hazard mapping: Papua New Guinea case study. British Geological Survey Technical Report WC/95/27
- Guthrie RH, Evans SG (2004a) Analysis of landslide frequencies and characteristics in a natural system, Coastal British Columbia. *Earth Surf Process Landforms* 29:1321–1339
- Guthrie RH, Evans SG (2004b) Magnitude and frequency of landslides triggered by a storm event, Loughborough Inlet, British Columbia. *Nat Hazard Earth Syst Sci* 4:475–483
- Guthrie RH, Evans SG (2007) Work, persistence, and formative events: the geomorphic impact of landslides. *Geomorphology* 88:266–275
- Guzzetti F, Arizzone F, Cardinali M, Galli M, Reichenbach P, Rossi M (2008) Distribution of landslides in the Upper Tiber River basin, central Italy. *Geomorphology* 96:105–122
- Guzzetti F, Malamud BD, Turcotte DL, Reichenbach P (2002) Power-law correlations of landslide areas in central Italy. *Earth Planet Sci Lett* 195:169–183
- Hergarten S, Neugebauer HJ (1998) Self-organized criticality in a landslide model. *Geophys Res Lett* 25:801–804
- Hovius N, Stark CP, Allen PA (1997) Sediment flux from a mountain belt derived by landslide mapping. *Geology* 25:231–234
- Hovius N, Stark CP, Chu HT, Lin JC (2000) Supply and removal of sediment in a landslide-dominated mountain belt: Central Range, Taiwan. *J Geol* 108:73–89
- Hungr D, Evans SG (2004) Entrainment of debris in rock avalanches: an analysis of a long run-out mechanism. *Geol Soc Am Bull* 116:1240–1252
- Hungr O, Evans SG, Harzard J (1999) Magnitude and frequency of rock falls and rock slides along the main transportation corridors of southwestern British Columbia. *Can Geotech J* 36:224–238
- Innes JL (1983) Lichenometric dating of debris-flow deposits in the Scottish Highlands. *Earth Surf Process Landforms* 8:579–588
- Jaquette C, Wohl E, Cooper D (2005) Establishing a context for river rehabilitation, North Fork Gunnison River, Colorado. *Environ Manag* 35:593–606
- Johnson KA, Sitar N (1990) Hydrologic conditions leading to debris-flow Initiation. *Can Geotech J* 27:789–801

- Jones KE, Preston NJ (2012) Spatial and temporal patterns of off-slope sediment delivery for small catchments subject to shallow landslides within the Waipaoa catchment, New Zealand. *Geomorphology* 141–142:150–159
- Junge WR (1978) Geologic hazards, North Fork Gunnison River Valley, Delta and Gunnison Counties, Colorado. Colorado Geological Survey, Open-File Report 78–12, explanation sheet, 6 maps
- Korup O (2005) Distribution of landslides in southwest New Zealand. *Landslides* 2:43–51
- Korup O (2006) Effects of large deep-seated landslides on hillslope morphology, western Southern Alps, New Zealand. *J Geophys Res Earth Surf* 111(F01018):18
- Larsen IJ, Montgomery DR, Korup O (2010) Landslide erosion controlled by hillslope material. *Nat Geosci* 3:247–251
- Lave J, Burbank D (2004) Denudation processes and rates in the Transverse Ranges, southern California: Erosional response of a transitional landscape to external and anthropogenic forcing. *J Geophys Res* 109(F01006):31
- Levy S, Jaboyedoff M, Locat J, Demers D (2012) Erosion and channel change as factors of landslides and valley formation in Champlain Sea Clays: the Chacoura River, Quebec, Canada. *Geomorphology* 145–146:12–18
- Lin G-W, Chen H, Shin T-Y, Lin S (2012) Various links between landslide debris and sediment flux during earthquake and rainstorm events. *J Asian Earth Sci* 54–55:41–48
- Locat P, Couture R, Leroueil S, Locat J, Jaboyedoff M (2006) Fragmentation energy in rock avalanches. *Can Geotech J* 43:830–851
- Malamud BD, Turcotte DL, Guzzetti F, Reichenbach P (2004) Landslide inventories and their statistical properties. *Earth Surf Process Landforms* 29:687–711
- Martin Y, Rood K, Schwab JW, Church M (2002) Sediment transfer by shallow landsliding in the Queen Charlotte Islands, British Columbia. *Can J Earth Sci* 39:189–205
- McClung DM (2000) Extreme avalanche runout in space and time. *Can Geotech J* 37:161–170
- Montgomery DR et al (1997) Hydrologic response of a steep, unchanneled valley to natural and applied rainfall. *Water Resour Res* 33:91–109
- Noever DA (1993) Himalayan sandpiles. *Phys Rev E* 47:724–725
- Palumbo L, Hetzel R, Tao M, Li X (2011) Catchment-wide denudation rates at the margin of NE Tibet from in situ-produced cosmogenic ¹⁰Be. *Terra Nova* 23:42–48
- Pelletier JD (1997) Kardar-Parisi-Zhang scaling of the height of the convective boundary layer and fractal structure of Cumulus cloud fields. *Phys Rev Lett* 78:2672–2675
- Regmi NR (2010) Hillslope dynamics in the Paonia–McClure Pass area, Colorado, USA. A dissertation submitted to the Department of Geology & Geophysics, Texas A&M University. <http://hdl.handle.net/1969.1/ETD-TAMU-2010-08-8573>
- Regmi NR, Giardino JR, McDonald, EV, Vitek JD (2013) A comparison of logistic regression-based models of susceptibility to landslides in western Colorado, USA. *Landslides*. doi:10.1007/s10346-012-0380-2
- Regmi NR, Giardino JR, Vitek JD (2010a) Modeling susceptibility to landslides using the weight of evidence approach: western Colorado. *Geomorphology* 115:172–187
- Regmi NR, Giardino JR, Vitek JD (2010b) Assessing susceptibility to landslides: using models to understand observed changes in slopes. *Geomorphology* 122:35–38
- Regmi NR, Giardino JR, Vitek JD, Briaud J-L (2007) Using immersive technology to map pre- and post-failure morphology of the Andy Gump landslide: Grand Mesa, Colorado, USA. *Geological Society of America, Abstracts with Programs* 39: 509
- Reichenbach P, Galli M, Cardinali M, Guzzetti F, Ardizzone F (2005) Geomorphologic mapping to assess landslide risk: concepts, methods and applications in the Umbria Region of central Italy. In: T. Glade, M.G. Anderson and M.J. Crozier (eds.) *Landslide hazard and risk*. Wiley, New York. pp. 429–468
- Roering JJ, Perron JT, Kirchner W (2007) Functional relationships between denudation and hillslope form and relief. *Earth Planet Sci Lett* 264:245–258
- Rogers WP (2003) Critical landslides of Colorado—a year 2002 review and priority list. Colorado Geological Survey, Open-File Report OF-02-16, 1map
- Schmidt KM, Montgomery DR (1995) Limits to relief. *Science* 270:617–620
- Sharp WD, Ludwig KR, Chadwick OA, Amundson R, Glaser LL (2003) Dating fluvial terraces by ²³⁰Th/U on pedogenic carbonate, Wind River Basin, Wyoming. *Quat Res* 59:139–150
- Silverman BW (1984) Spline smoothing—the equivalent variable kernel-method. *Ann Stat* 12:898–916
- Simonett DS (1967) Landslide distribution and earthquakes in the Bewani and Torricelli Mountains, New Guinea. In: J.N. Jennings and J.A. Mabutt (eds.) *Landform studies from Australia and New Guinea*. Cambridge University Press, Cambridge. pp. 64–84
- Sinnock S (1981) Pleistocene drainage changes in Uncompaghe Plateau-Grand Valley region of western Colorado, including formation and abandonment of Unaweep Canyon: a hypothesis. *N M Geol Soc Guideb* 32:127–136
- Somfai E, Czirik A, Vicssek T (1994) Power-law distribution of landslides in an experiment on the erosion of a granular pile. *J Phys A Math Gen* 27:L757–L763
- Stark CP, Guzzetti F (2009) Landslide rupture and the probability distribution of mobilized debris volumes. *J Geophys Res Earth Surf* 114(F00A02):16
- Stark CP, Hovius N (2001) The characterization of landslide size distributions. *Geophys Res Lett* 28:1091–1094
- Western Regional Climate Center (2012) <http://www.wrcc.dri.edu/cgi-bin/cliMAIN.pl?copaon>
- Whitehouse IE, Griffiths GA (1983) Frequency and hazard of large rock avalanches in the Central Southern Alps, New-Zealand. *Geology* 11:331–334
- Wilson CJ, Dietrich WE (1987) The contribution of bedrock groundwater flow to storm runoff and high pore pressure development in hollows. In: Beschta RL, Blinn T, Grant GE, Ice G, Gand Swanson FJ (Eds.) *Erosion and Sedimentation in the Pacific Rim, International, Association of Hydrological Sciences*, pp. 49–60
- Wise S (2000) Assessing the quality for hydrological applications of digital elevation models derived from contours. *Hydrol Process* 14:1909–1929
- Wolman MG, Miller JP (1960) Magnitude and frequency of forces in geomorphic processes. *J Geol* 68:54–74

N. R. Regmi

Division of Earth and Ecosystem Sciences, Desert Research Institute, Reno, NV 89512, USA

N. R. Regmi (✉) · J. R. Giardino · J. D. Vitek

HAARP (High Alpine and Arctic Research Program) and Department of Geology and Geophysics, Texas A&M University, College Station, TX 77843, USA
e-mail: regminr@dri.edu